Serine 105 and 120 are important phosphorylation sites for porcine reproductive and respiratory syndrome virus N protein function

Yao Chen[a,b,c], Xiulin Xing[a,b,c], Qi Li[a,b,c], Songlin Feng[a,b,c], Xiaoliang Han[a,b,c], Shuyi He[a,b,c], Guihong Zhang[a,b,c,*]

[a] Key Laboratory of Zoonosis Prevention and Control of Guangdong Province, College of Veterinary Medicine, South China Agricultural University, Guangzhou, China
[b] College of Veterinary and National Engineering Research Center for Breeding Swine Industry, South China Agricultural University, Guangzhou, China
[c] National and regional Joint Engineering Laboratory for Medicament of Zoonosis Prevention and Control, China

A B S T R A C T

The nucleocapsid (N) protein is the most abundant protein of porcine reproductive and respiratory syndrome virus (PRRSV). It has been shown to be multiphosphorylated. However, the phosphorylation sites are still unknown. In this study, we used liquid chromatography tandem mass spectrometry (LC–MS/MS) to analyze the phosphorylation sites of N protein expressed in Sf9 cells. The results showed that N protein contains two phosphorylation sites. Since N protein can regulate IL-10, which may facilitate PRRSV replication, we constructed four plasmids (pCA-XH-GD, pCA-A105, pCA-A120 and pCA-A105-120) and transfected them into Pig alveolar macrophages (PAMs,3D4/2). The qPCR results showed that mutations at residues 105 and 120 were associated with down-regulation of the IL-10 mRNA level, potentially decreasing the viral growth ability. Then, we mutated the phosphorylation sites (S105A and S120A) and rescued three mutated viruses, namely, A105, A120 and A105-120. Compared with wild-type virus titers, the titers of the mutated viruses at 48 hpi were significantly decreased. The Nsp(non-structural protein) 9 qPCR results were consistent with the multistep growth kinetics results. The infected PAMs (primary PAMs) results were similar with Marc-145.The findings indicated that the mutations impaired the viral replication ability. The confocal microscopy results suggested that mutations to residues 105 and 120 did not affect N protein distribution. Whether the mutations affected other functions of N protein and what the underlying mechanisms are need further investigation. In conclusion, our results show that residues 105 and 120 are phosphorylation sites and are important for N protein function and for viral replication ability.

1. Introduction

Porcine reproductive and respiratory syndrome virus (PRRSV) is an enveloped, positive-stranded virus (Kvisgaard et al., 2017). PRRSV, lactate dehydrogenase-elevating virus (LDV), simian hemorrhagic fever virus (SHFV), and equine arteritis virus (EAV) are members of family *Arteriviridae*. PRRSV has two types: the EU type and the NA type (Xie et al., 2017). PRRSV contains 14 non-structural proteins and 7 structural proteins (Chen et al., 2016).

The nucleocapsid (N) protein, which is the most abundant protein in the virus particle, is a 15 kD protein (Doan and Dokland, 2003) of 123 or 128 aa. The N protein is important for virus assembly (Snijder et al., 2013). It can regulate IL-10 and enhance regulatory T lymphocyte proliferation, when residues 15 and 46 are mutated (Fan et al., 2015). N also has been found to be connected with Nsp9, Nsp10 and viral RNA

(Chen et al., 2017; Liu et al., 2016; Wang et al., 2012). The N protein has been proven to be multiphosphorylated (Wootton et al., 2002). Moreover, the serine 120 was proven to be a phosphorylation site that, if mutated,impairs viral growth ability (Liu et al., 2017). The other modifications of the N protein are still unknown.

Knowledge of the modifications of N protein are fundamental to understanding the PRRSV life cycle. However, the post-translational and other modification sites of N protein are still unclear, especially the phosphorylation sites. To date, mass spectrometry has proved to be a powerful tool in the analysis of protein phosphorylation sites (Bittremieux et al., 2017). Since N protein is difficult to purify from virions (Chen et al., 2005), in this research, a baculovirus expression system, which is widely used in analyzing post-translational protein modifications, was used to express the N protein (Peng et al., 2012; Zhang et al., 2017). We used liquid chromatography tandem mass

Table 1
The primers used in this study.

| Name	Sequence (5′-3′)
pFast-N-F	CCGCTCGAGCCACCATGGCAAATAACAACGGCAAG
pFast-N-R	CGGGGTACCTAGTGATGGTGATGGTGGTGTGCTGAG
	GGTGATGCTGTGGCGCGGATCAG
A105-F	AGTTACACTGTGGAGTTTGCATTGCCGACGCAACATACTG
A105-R	GATCAGACGCACAGTATGTTGCGTCGGCAATGCAAACTCC
A120-F	AACTGCATGTCCTGGCGCTA
A120-R	GAATGCCAGCCCATCATGCTGAGGGTGCTGC
D-F	CACATTGGTGCCCGGGTTGA
D-R	GGGATCGAGGTACCCAGAAGC
RT-Nsp9-F	CCCTCCATGCCAAACTACCAC
RT-Nsp9-R	TTGTCTTCTTTGGGTCCGTCT
GAPDH-F	GCAAAGACTGAACCCACTAATTT
GAPDH-R	TTGCCTCTGTTGTTACTTGGAGAT
IL-10-F	TTCAAACGAAGGACCAGATG
IL-10-R	CACAGGGCAGAAATTGATGA
β-actin -F	AGGAAGGAGGGCTGGAAGAG
β-actin-R	GCGGGACATCAAGGAGAAG
pCA-F	CCCATCGATGCCACCATGGCAAATAACAACGGCAAGCAGCAAAAG
pCA-A105R	CCGCTCGAGTCAATGATATGATGATGATGTGCTGAGGGTGATGCTGTGGCGCGGATCA
pCA-A120R	CCGCTCGAGTCAATGGTGATGGTGATGATGTGCTGAGGGTGCTGCTGTGGCGCGGATCA
RT-N-F	AACCAGTCCAGAGGCAAGG
RT-N-R	GACAGGGCACAAGTTCCAG
IL-12 p40-F	GGGTGGGAACACAAGAGAT
IL-12 p40-R	GGCTAAACTTGCCTAGAGGT
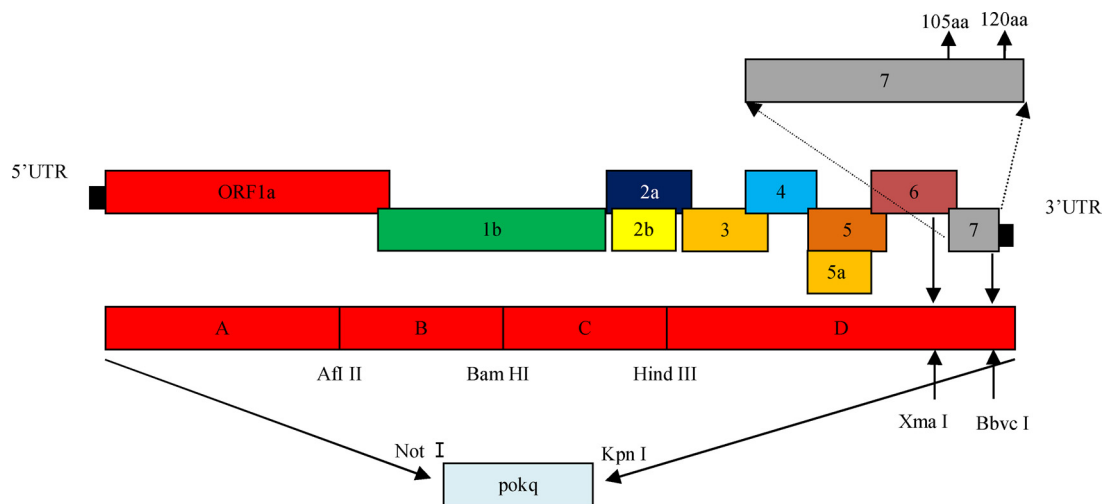
Fig. 1. The schematic diagram of PRRSV infectious clones.
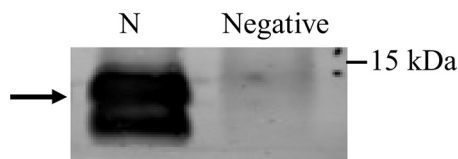
Fig. 2. Purified recombinant N protein expressed in Sf9 cells. The results of Ni-chelating affinity chromatography. The position of the PRRSV N protein is marked by an arrow.

spectrometry (LC–MS/MS) to identify the modification sites of N protein expressed in Sf9 cells. The analysis achieved 85% coverage of the N protein and identified two phosphorylation sites, namely, residues 105 and 120. Our results show that residue 105 is a phosphorylation site and that residues 105 and 120 are important for N protein function.

2. Materials and methods

2.1. Virus and cells

Sf9 cells were maintained in SF900[TM] SFM II medium (Gibco, USA) at 27 °C. PAMs (ATCC,3D4/2) (Yu et al., 2017), PAMs (primary PAMs) and Marc-145 cells were cultured in Dulbecco's modified Eagle's medium (DMEM, Gibco), supplemented with 10% fetal bovine serum (FBS, BI, Israel) at 37 °C in 5% CO_2. XH-GD (GenBank accession no. EU624117.1) was used in the virus infection studies.

2.2. Plasmid construction and DNA transfection

To synthesize the recombinant PRRSV N protein from Sf9 cells, the N genes of XH-GD were amplified with specific primers (Table 1) and cloned into the pFastBac Dual vector (Invitrogen, USA) or pCAGGS-MCS vector. The forward primers contained a Kozak sequence, and the

Table 2
Summary of the predicted phosphorylation sites in the PRRSV N protein.

Amino acid	Net phos (*in silico*) prediction value[a]	LC–MS/MS Phosphorylation score[b]
36S	**0.681**	ND
59T	**0.638**	ND
68T	**0.936**	ND
70s	**0.673**	ND
77s	**0.673**	ND
78s	**0.500**	ND
81T	0.494	ND
89T	0.474	ND
93S	0.481	ND
95S	0.479	ND
99S	**0.989**	0.62
100Y	**0.555**	ND
101T	0.487	0.62
105S	**0.569**	**0.01166**
108T	0.454	ND
111T	**0.607**	0.35
118T	**0.550**	ND
120S	**0.830**	**0.004188**
122s	0.455	ND

[a] The NetPhos 3.1 server (http:/www.cbs.dtu.dk/services/NetPhos/%20) was used to predict the PRRSV N protein phosphorylation. Phosphorylation is likely for residues with values > 0.5, which are shown in bold.

[b] Likely phosphorylation if score < 0.05. ND, not detected.

reverse primers contained a 6 × His Tag. Recombinant baculoviruses were obtained using the Bac-to-Bac Baculovirus Expression System (Invitrogen, USA) according to the manufacturer's protocol. The cells were collected at 72 h post-transfection (Fan et al., 2015). For transfection of PAMs(3D4/2), the cell were spilt into 6-well plate. Plasmids (pCA-XH-GD, pCA-A105, pCA-A120 and pCA-A105-120) were individually transfected into cells at 2 µg each. Transfection was performed with Lipofectamine™ 3000 (Invitrogen), and cells were incubated for 48 h. The control group was transfected with empty vector only (Yu et al., 2017).

2.3. Western blot

Cells were lysed in RIPA lysis buffer (Beyotime Biotechnology, China) with a protease inhibitor cocktail (Thermo Fisher, USA). Bradford assays were used to quantify the protein contents. A total of 5 µg of protein was separated by SDS-PAGE (15%) and transferred to a nitrocellulose membrane (Millipore, USA). The membrane was blocked for 1 h in phosphate-buffered saline (TBST) plus 5% milk (BD, USA). N monoclonal antibody (SDOW17,Median, South Korea) was diluted 1:1000 in TBST and incubated with the membrane overnight. The membrane was washed three times in TBST. Then, the membrane was incubated with goat anti-mouse secondary antibody (LI-COR Biosciences, USA) for 1 h in the dark at 37 °C. The membrane was washed three times with TBST. Then, the membrane was analyzed by using an Odyssey Infrared Imaging System (LI-COR Biosciences, USA) (Xie et al., 2014; Hu et al., 2017). The samples were stored at −80 °C.

2.4. Protein purification and mass spectrometry

The purification process was carried out according to the manufacturer's protocol. Briefly, the lysate (pH = 8) was incubated with Q Sepharose Fast Flow (GE Healthcare, USA) for 2 h at 25 °C, and the filtrate was then collected. Subsequently, the filtrate was incubated with Ni Sepharose 6 Fast Flow (GE, USA) for 2 h at 25 °C. Then, the filtrate was washed with increasing concentrations of imidazole (60 and 100 mM imidazole, 25 mM Tris, 500 mM NaCl, pH = 7.4). Finally, the sample was washed with elution buffer (25 mM Tris, 500 mM NaCl, 500 mM imidazole, pH = 7.4) (Fan et al., 2015). The sample was

separated using 15% SDS-PAGE, and the target bands were analyzed by LC–MS/MS (Zhang et al., 2017). The LC–MS/MS results were analyzed by Proteome Discoverer (Thermo Fisher, USA)

2.5. Real-time PCR

According to the manufacturer's instructions, total RNA was extracted with TRIzol reagent(Invitrogen, USA). MLV (Takara, Japan) was used to synthesize the cDNA. Real-time PCR was performed on the CFX96™ Real-Time System (Bio-Rad, USA). The primers and calculated method were the same as in the previous report (Xie et al., 2014; Yu et al., 2017).

2.6. Recombinant virus rescue

The PRRSV infectious clones were similar to those from a previous report (Zhang et al., 2013). The schematic diagram were shown in the Fig. 1.The infectious clones were constructed by the fusion PCR. The three mutated plasmids (pokXH-GDA105, pokXH-GDA120, pokXH-GDA105-120)were individually transfected into BHK-21 cells. Transfection was performed with Lipofectamine™ 3000 (Invitrogen) according to the manufacturer's protocol. The cells were collected at 48 h post-transfection as the primary passage (P0). Then, Marc-145 cells were infected by the P0 virus for three passages (P1-P3). The mutations in the rescued virus were confirmed by RT-PCR and sequencing (Zhang et al., 2013).

2.7. Confocal microscopy

The Marc-145 cells were infected with individual mutant viruses. At 48 h post-infection (hpi), the cells were fixed in methanol, washed five times with PBS and incubated at 4 °C overnight with monoclonal antibody against the N protein (Median, South Korea) (1:400 dilution). Subsequently, the cells were washed in PBS five times and then incubated with fluorescein isothiocyanate (FITC)-conjugated anti-mouse IgG (1:100 dilution) for 1 h at 37 °C. Finally, the cells were incubated with DAPI (4′,6-diamidino-2-phenylindole, Thermo Fisher, USA) for 15 min at 37° C (Xie et al., 2014). Fluorescence was observed using a laser scanning confocal microscope (Olympus, Japan).

2.8. Multistep growth curve

The multistep growth curve assay was performed as previously reported. Briefly, the Marc-145 cells were infected by P3 at a multiplicity of infection (MOI) of 0.1. The supernatants were collected at certain time points (12, 24, 36, 48, 60, 72 and 84 h) post-infection. The viral titer was measured in the Marc-145 cells. The results were calculated using the Reed-Muench method (Xie et al., 2014).

2.9. Data analysis

Data were analyzed as the means ± standard deviations (SD) of three independent experiments. Statistical analyses were done using SPSS software (version 21.0). Tukey's test was used to evaluate the differences among the groups, and a *p* value < 0.05 was considered statistically significant.

3. Results

3.1. Expression and purification of N protein from Sf9 cells

Since it is difficult to purify the N protein from virions (Chen et al., 2005), baculovirus expression systems, which are extensively applied in expressing recombinant proteins (Zhang et al., 2017), were used to express the recombinant N protein and confirmed by western blotting with N antibody. To achieve greater protein purity, lysates were first
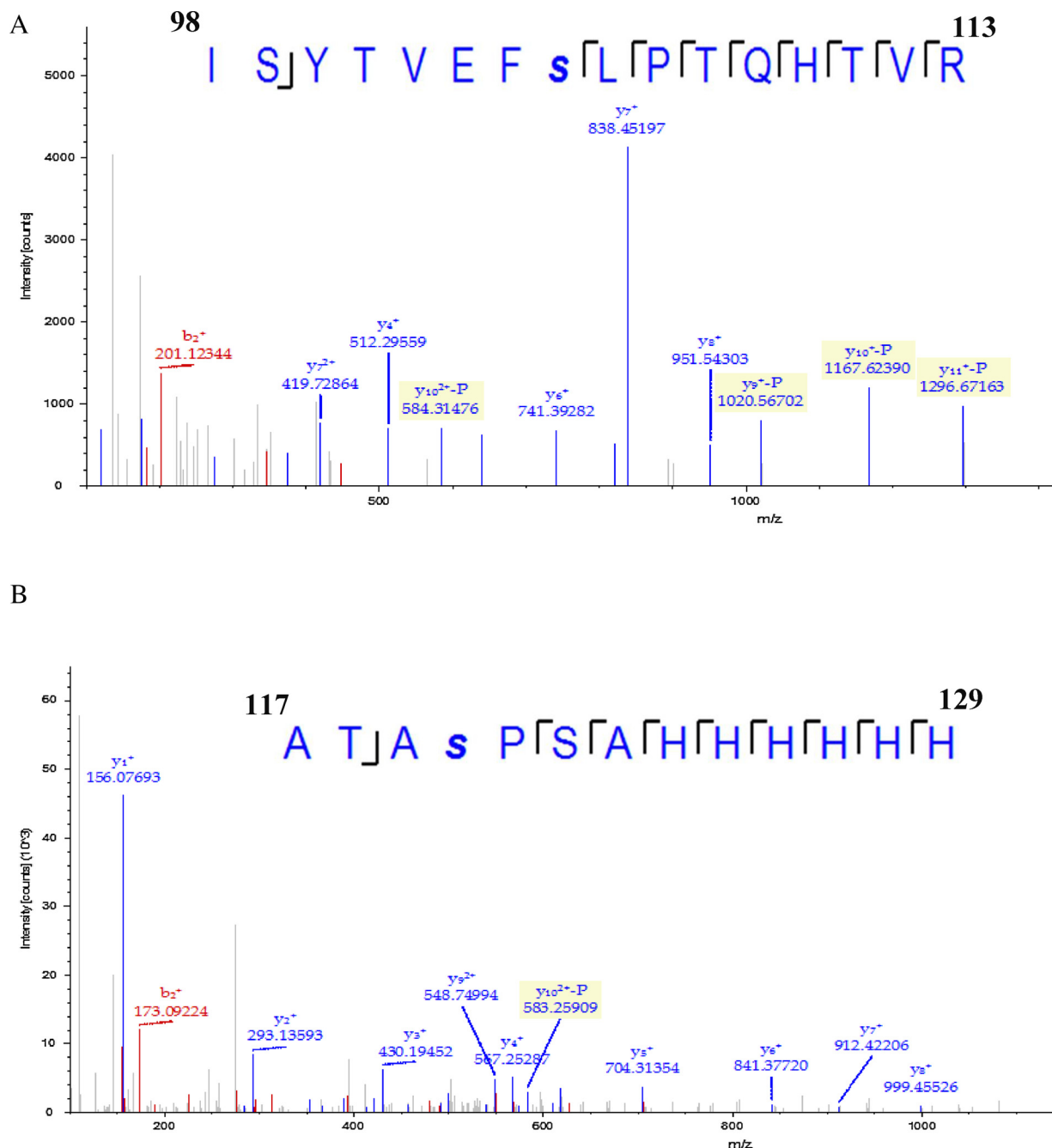
Fig. 3. Mapping PRRSV N protein phosphorylation sites by mass spectrometry. N protein was digested by either trypsin or chymotrypsin. (A) Spectra derived from the N protein peptide aa98–113 identified phosphorylated S105 residues. (B) Spectra derived from the N protein peptide aa117–129 identified phosphorylated S120 residues. Lowercase indicates the phosphorylation site.

isolated with ion exchange chromatography. Then, the filtrate was incubated with Ni Sepharose 6 Fast Flow (Fig. 2). The purification process was performed with reference to the operation manual. Due to degradation, the proteins appeared as two bands after the purification. Both bands were the PRRSV N protein (data no shown).

3.2. In silico modeling and identification of residue 105 as a phosphorylation site in the N recombinant protein

Since the N protein has proven to be a multiphosphorylated protein, Netphos3.1 (http:/www.cbs.dtu.dk/services/NetPhos/%20) was used to identify the potential N protein phosphorylation sites (Blom et al., 1999; Zengel et al., 2015). Twelve sites were predicted as potential

phosphorylation sites (Table 2).

Each phosphorylation group results in a mass increase. To identify the phosphorylation sites in PRRSV N protein, the purified protein was analyzed by LC–MS/MS (Thermo Fisher, USA) to yield a moiety of an m/z of 98 Da (H_3PO_4 or HPO_3). The protein was digested by either trypsin or chymotrypsin to yield smaller peptide fragments. The results show that the identified peptides encompass approximately 85.7% of the 129 amino acids of the recombinant protein. As shown in Fig. 3, by comparison with the theoretical masses, we found two phosphorylation sites. All the sites were located at the C terminus of the N protein. Residue 120 was shown to be phosphorylated in previous research (Han and Yoo, 2014).
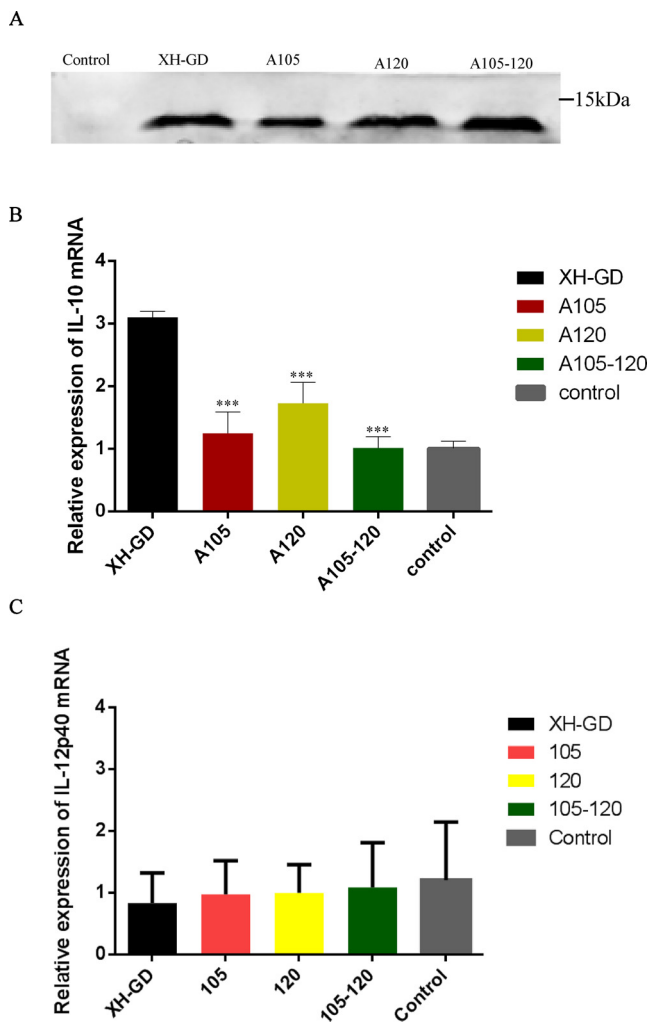
A

B

C

Fig. 4. The mutation could decrease the IL-10 mRNA level. (A) Western blotting results. PAM (3D4/2) cells were cultivated in a 6-well plate and transfected with 2 μg plasmid. Forty-eight hours post-transfection, the cells were lysed by RIPA lysis buffer. The results showed that N protein could be detected in all samples. (B,C) Total RNA was extracted and subjected to real-time PCR analysis. The fold change in IL-10 gene levels(B) or IL-12p40mRNA (C)compared to β-actin were determined. The data shown represent the mean ± SD ($n = 3$) (*, $P < 0.05$; **, $P < 0.01$; ***, $P < 0.001$ in comparison with the XH-GD group).
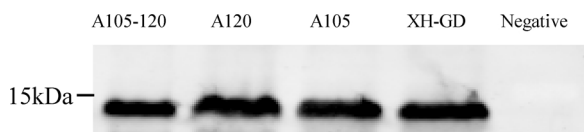

Fig. 5. Western blotting results. The cells were cultivated in a 6-well plate and incubated with virus. Forty-eight hours post-infection, the cells were lysed by RIPA lysis buffer. The results show that all samples contain the N protein, indicating that all the mutant viruses could be rescued.

3.3. The mutations could down-regulate the N-induced IL-10 mRNA

N protein has many functions, such as nuclear localization, upregulation of IL-10 and virus assembly. IL-10 is a pleiotropic cytokine that may facilitate PRRSV replication (Song et al., 2013). Since it has been proven that the N protein can up-regulate IL-10 (Liu et al., 2015), we constructed four plasmids (pCA-XH-GD, pCA-A105, pCA-A120 and pCA-A105-120) and transfected them into PAMs as previously reported (Yu et al., 2017). Their expression were verified by western blotting

(Fig. 4A). Real-time PCR showed that N protein dephosphorylation down-regulated the IL-10 mRNA level; the IL-10 mRNA level of cells transfected with A105-120 was the lowest observed (Fig. 4B). according to the previous research (Yu et al., 2017),we also detected the IL-12 p40 mRNA level. As shown in the Fig. 4C, There were not significantly different between the viruses.

3.4. N protein phosphorylation did not affect viral viability and infectivity

According to previous reports, Mutated residue 120 of N protein did not affect viral infectivity and viability (Liu et al., 2017). However, we found that reside 120 was not a conserved site and that the deletion of residue 120 did not affect virus viability (Tan et al., 2011). To study the function of the phosphorylation sites, three mutant plasmids were constructed, namely, pokXH-GDA105 (S105A), pokXH-GDA120 (S120A) and pokXH-GDA105-120 (S015A, S120A). The plasmids were transfected into BHK-21 cells. The cells were collected and passaged in Marc-145 cells for up to three passages. The sequencing results confirmed that the substitutions were stable in the three mutant viruses. The western blotting results show that all mutated viruses expressed the N protein at 48 hpi (Fig. 5). The results indicated that the mutations did not affect the recovery of PRRSV.

3.5. The phosphorylation of N protein impaired viral growth

A previous report showed that residue 120 was important for the viral replication ability (Liu et al., 2017). Therefore, we questioned whether alteration of residue 105 would also affect the viral growth ability. Multistep growth kinetics were measured in infected Marc-145 cells in three independent experiments. Viral titers were determined by TCID$_{50}$. The wild-type virus reached a peak titer at 48 hpi. The other viruses reached peak titers at 60 hpi. The wild-type virus showed a stronger growth ability than the mutated viruses. There were significant differences between the wild-type virus and A105, A120 and A105-120 viruses at 48 hpi (Fig. 6A). Compared with the A105 and A120, A105-120 showed lower viral growth. For quantitative analysis of PRRSV, total RNA was extracted for real-time PCR as previously reported (Xie et al., 2014). The real-time PCR results showed that the Nsp9 gene level was lowest in A105-120 (Fig. 6B). Then,the PAMs(primary PAMs) were infected with 0.1MOI PRRSV. At 48 hpi, total RNA was extracted for real-time PCR. The results were similar with the Marc-145, the mutation reduce the viral gene level (Fig. 7A),but did not impaired the IL-10 mRNA level (Fig. 7B). These results mirror those of the multistep growth kinetics. This finding indicated that residue 105 could affect viral growth, similarly to residue 120, and that the phosphorylation of N may play an important role in the virus life cycle.

3.6. Mutation of residues 105 and 120 did not affect the N protein distribution in cells

Because residue 105 and residue 120 are close to the N protein nuclear export signal (Han and Yoo, 2014), we wished to further investigate whether these mutations would affect the N protein distribution in cells. The Marc-145 cells were incubated with A105-120 and wild-type virus at 0.1 MOI. The N protein signal was examined using an indirect immunofluorescence assay (Fig. 8). N protein was detected in the cytoplasm and nuclei. There are not significant differences in the localization of A105-120 and wild-type virus. This finding indicated that the mutations did not interfere in N protein distribution.

4. Discussion

Post-translational modification is important for protein function (Bittremieux et al., 2017). As an abundant protein in PRRSV, N protein has been proven to have many functions, including regulation of host cytokines, connection with other viral proteins and so on (Liu et al.,
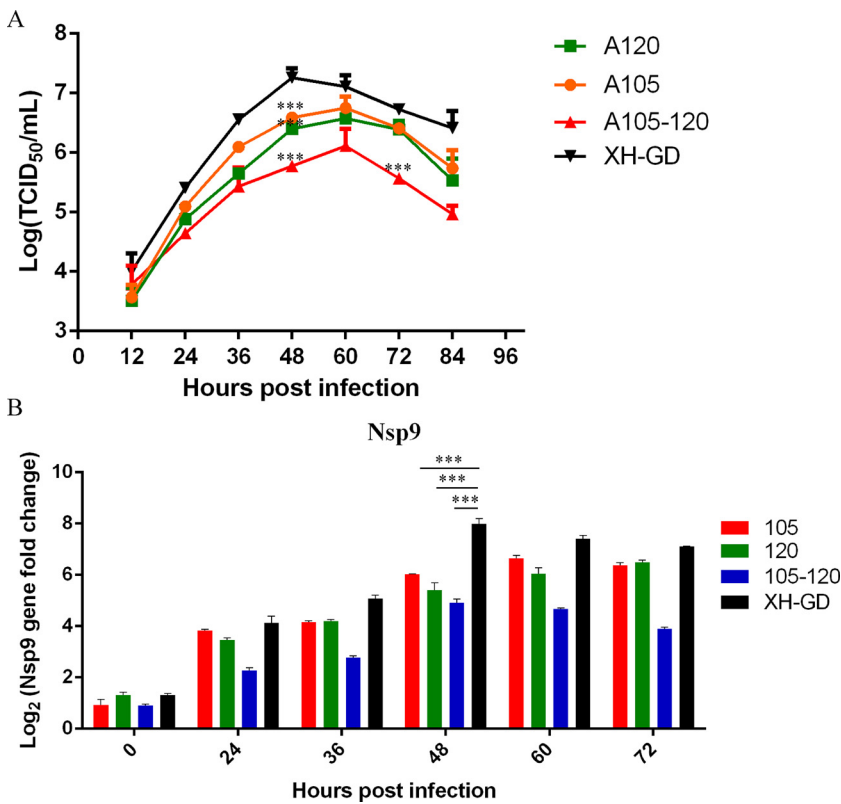
Fig. 6. Virological characteristics of the N protein mutants. (A) Multistep kinetics of mutant viruses and wild-type virus in Marc-145 cells. Cells were infected with PRRSV at MOI 0.1. The supernatants were collected at various time points and titrated. The $TCID_{50}$ was calculated by the Reed-Muench method. (B) Total RNA was extracted and subjected to the real-time PCR analysis, and the fold change in PRRSV Nsp9 gene levels compared with GAPDH was determined. The data shown represent the mean ± SD ($n = 3$) (*, $P < 0.05$; **, $P < 0.01$; ***, $P < 0.001$ in comparison with the XH-GD group).

2016; Han and Yoo, 2014). However, the modification of the N protein are still unclear, especially the phosphorylation sites. Determining the modifications of the N protein would be helpful for understanding the life cycle of PRRSV.

As a protein modification, phosphorylation is important for regulating protein function and virus biology. In this study, we found two phosphorylation sites by LC–MS/MS, including Ser105 and Ser120. We confirmed that the N protein was a multiphosphorylated protein, as previously reported (Wootton et al., 2002).

There are many viruses, such as PRRSV, SARS and IBV, contain the nucleocapsid proteins that have been proven to be phosphorylated proteins. Many of these nucleocapsid proteins were found to play a vital function during the viral life cycle, such as in mumps virus or Hanta virus (Zengel et al., 2015). Since the N protein could up-regulate IL-10, according to previous research (Yu et al., 2017), PAMs were transfected with four plasmids. The qPCR results suggested that the mutation down-regulated the induction of IL-10 mRNA. However, the IL-10 mRNA qPCR result of infected PAMs were different with the transfected PAMs.One possible reason is that the other proteins, such as GP5 and Nsp9, could regulate the IL-10 (Burgara-Estrella et al., 2013).

Previous reports have demonstrated that Ser120 did not affect the recovery of virus (Liu et al., 2017; Tan et al., 2011). However, when comparing the different strains, we found that residue 105 was more conserved than residue 120 (Fig. 9). This indicates that residue 105 may be a major phosphorylation site. Therefore, we substituted Ser105 and Ser120 with Ala individually and together. The three mutant viruses were rescued from Marc-145 cells. It is indicated that the phosphorylation of N protein may not be essential for the viability of PRRSV. Mutated the N phosphorylation sites could decrease the viral titier, it is proved that the mutations could impair the viral replication ability (Fig. 6).

According to previous reports, there are three functions of N protein phosphorylation, which may fall into the categories of modulating its nuclear localization, regulating host cytokines and regulating the protein's binding to viral RNA (Liu et al., 2015; Wootton et al., 2002). Our
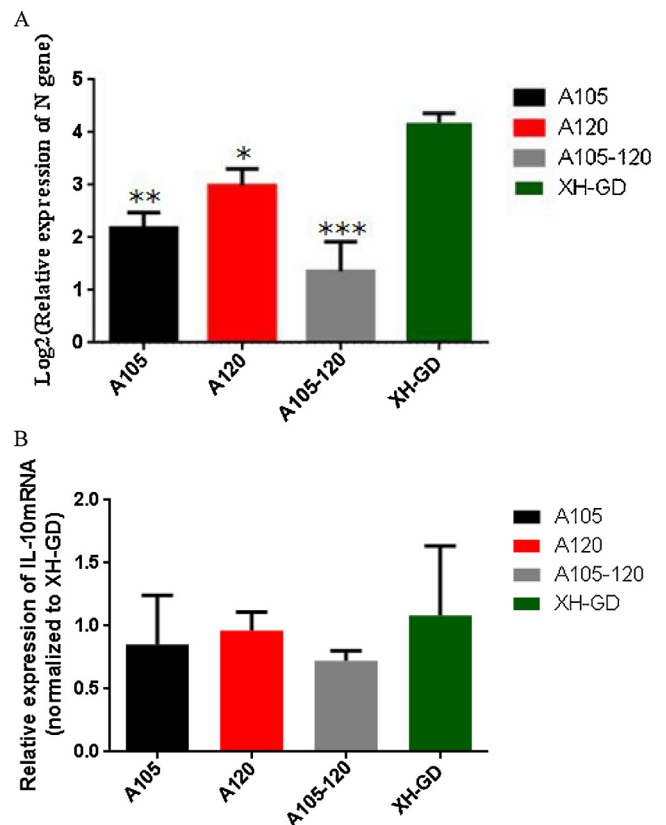
Fig. 7. The qPCR result of infected PAMs. Cells were infected with PRRSV at MOI 0.1.Total RNA was extracted at 48h post-infection and subjected to the real-time PCR analysis, (A) The fold change in PRRSV N gene levels level compared with βoactin was determined;(B) Level of IL-10 mRNA production was calculated after normalization to pokXH-GD.The data shown represent the mean ± SD ($n = 3$) (*, $P < 0.05$; **, $P < 0.01$; ***, $P < 0.001$ in comparison with the XH-GD group).

Fig. 8. Marc-145 cells infected with A105-120 or XH-GD at an MOI of 0.1. At 48 hpi, the infected cells were fixed with PBS and incubated with mouse anti-N mAb, followed by FITC goat anti-mouse IgG (H + L).The nuclei were stained with DAPI.

Fig. 9. Amino acid sequence alignments of the N protein from isolates that are available in the National Center for Biotechnological Information (NCBI) database. Residues 105 and 120 are shown in brown and red. (For interpretation of the references to colour in this figure legend, the reader is referred to the web version of this article).

results showed that the mutations did not change the distribution of N protein in infected cells. The poor growth ability may be related to host cytokine activity or protein binding activity to viral RNA. In terms of binding activity to viral RNA, as we know, the modifications and structure of the PRRSV N protein are similar to those of *Coronavirus* (Chang et al., 2005). It is possible that they have the similar mechanism. In the case of IBV or MHV, the phosphorylated N protein may have a higher binding affinity than the unphosphorylated N protein for genomic RNA (Spencer et al., 2008). Therefore, we speculated that the phosphorylation modification may help N protein to bind to viral RNA, and hence the mutation to the phosphorylated residue would decrease this binding. However, the mechanism underlying the poor growth ability of these mutants still needs further investigation.

In conclusion, through a combination of affinity purification and LC–MS/MS, our results show that N protein expressed in insect cells contains two phosphorylation sites, including one novel phosphorylation site. Our qPCR results showed that constitutive dephosphorylation decreases the N-induced expression of IL-10 mRNA in transfected PAMs. Utilizing reverse genetics, we found that Ser105 and Ser120 did not affect virus infection and viability but does play a role in viral growth. Those findings indicated that phosphorylation at these sites affects N protein functions. The mechanism needs further investigation. Since the MS/MS method has shortcomings, other possible phosphorylation sites within the N protein cannot be ruled out. These studies will be helpful for understanding the role of the N protein in the PRRSV life cycle.

Author contributions

Designed experiments: YC. Performed the experiments: YC, XX, QL,

SF. Analyzed the data: XH, SH. Wrote the manuscript: YC. Revised the manuscript: GZ, XH.

Conflict of interest

The authors declare no conflicts of interest.

Acknowledgements

References

Bittremieux, W., Tabb, D.L., Impens, F., Staes, A., Timmerman, E., Martens, L., Laukens, K., 2017. Quality control in mass spectrometry-based proteomics. Mass Spectrom. Rev. http://dx.doi.org/10.1002/mas.21544.

Blom, N., Gammeltoft, S., Brunak, S., 1999. Sequence and structure-based prediction of eukaryotic protein phosphorylation sites. J. Mol. Biol. 294, 1351–1362.

Burgara-Estrella, A., Diaz, I., Rodriguez-Gomez, I.M., Essler, S.E., Hernandez, J., Mateu, E., 2013. Predicted peptides from non-structural proteins of porcine reproductive and respiratory syndrome virus are able to induce IFN-gamma and IL-10. Viruses 5, 663–677.

Chang, C.K., Sue, S.C., Yu, T.H., Hsieh, C.M., Tsai, C.K., Chiang, Y.C., Lee, S.J., Hsiao, H.H., Wu, W.J., Chang, C.F., Huang, T.H., 2005. The dimer interface of the SARS coronavirus nucleocapsid protein adapts a porcine respiratory and reproductive syndrome virus-like structure. FEBS Lett. 579, 5663–5668.

Chen, H., Gill, A., Dove, B.K., Emmett, S.R., Kemp, C.F., Ritchie, M.A., Dee, M., Hiscox, J.A., 2005. Mass spectroscopic characterization of the coronavirus infectious bronchitis virus nucleoprotein and elucidation of the role of phosphorylation in RNA binding by using surface plasmon resonance. J. Virol. 79, 1164–1179.

Chen, X., Zhang, Q., Bai, J., Zhao, Y., Wang, X., Wang, H., Jiang, P., 2017. The Nucleocapsidnucleocapsid protein and nonstructural protein 10 of highly pathogenic porcine reproductive and respiratory syndrome virus enhance CD83 production via NF-kappaB and Sp1 signaling pathways. J. Virol. 91.

Chen, Y., He, S., Sun, L., Luo, Y., Sun, Y., Xie, J., Zhou, P., Su, S., Zhang, G., 2016. Genetic variation, pathogenicity, and immunogenicity of highly pathogenic porcine reproductive and respiratory syndrome virus strain XH-GD at different passage levels. Arch. Virol. 161 (1), 77–86.

Doan, D.N., Dokland, T., 2003. Cloning, expression, purification, crystallization and preliminary X-ray diffraction analysis of the structural domain of the nucleocapsid N protein from porcine reproductive and respiratory syndrome virus (PRRSV). Acta Crystallogr. D Biol. Crystallogr. 59, 1504–1506.

Fan, B., Liu, X., Bai, J., Li, Y., Zhang, Q., Jiang, P., 2015. The 15N and 46R residues of highly pathogenic porcine reproductive and respiratory syndrome virus nucleocapsid protein enhance regulatory T lymphocytes proliferation. PLoS One 10, e138772.

Han, M., Yoo, D., 2014. Engineering the PRRS virus genome: updates and perspectives. Vet. Microbiol. 174, 279–295.

Hu, P., Chen, X., Huang, L., Liu, S., Zang, F., Xing, J., Zhang, Y., Liang, J., Zhang, G., Liao, M., Qi, W., 2017. A highly pathogenic porcine reproductive and respiratory syndrome virus candidate vaccine based on Japanese encephalitis virus replicon system. PeerJ 5, e3514.

Kvisgaard, L.K., Larsen, L.E., Hjulsager, C.K., Botner, A., Rathkjen, P.H., Heegaard, P., Bisgaard, N.P., Nielsen, J., Hansen, M.S., 2017. Genetic and biological characterization of a porcine reproductive and respiratory syndrome virus 2 (PRRSV-2) causing significant clinical disease in the field. Vet. Microbiol. 211, 74–83.

Liu, H., Jiang, Y., Huang, Q., Yang, S., Zhang, W., Yu, L., Gao, F., Zhou, Y., Tong, G., 2017. Identification and functional analysis of the phosphorylation site of porcine reproductive and respiratory syndrome virus nucleocapsid protein. Chin. J. Prev. Vet. Med. 39 (7), 518–523.

Liu, L., Tian, J., Nan, H., Tian, M., Li, Y., Xu, X., Huang, B., Zhou, E., Hiscox, J.A., Chen, H., 2016. Porcine reproductive and respiratory syndrome virus nucleocapsid protein interacts with Nsp9 and cellular DHX9 to regulate viral RNA synthesis. J. Virol. 90, 5384–5398.

Liu, X., Fan, B., Bai, J., Wang, H., Li, Y., Jiang, P., 2015. The N-N non-covalent domain of the nucleocapsid protein of type 2 porcine reproductive and respiratory syndrome virus enhances induction of IL-10 expression. J. Gen. Virol. 96, 1276–1286.

Peng, Z., Liao, Z., Dziegielewska, B., Matsumoto, Y., Thomas, S., Wan, Y., Yang, A., Tomkinson, A.E., 2012. Phosphorylation of serine 51 regulates the interaction of human DNA ligase I with replication factor C and its participation in DNA replication and repair. J. Biol. Chem. 287, 36711–36719.

Snijder, E.J., Kikkert, M., Fang, Y., 2013. Arterivirus molecular biology and pathogenesis. J. Gen. Virol. 94, 2141–2163.

Song, S., Bi, J., Wang, D., Fang, L., Zhang, L., Li, F., Chen, H., Xiao, S., 2013. Porcine reproductive and respiratory syndrome virus infection activates IL-10 production through NF-kappaB and p38 MAPK pathways in porcine alveolar macrophages. Dev. Comp. Immunol. 39, 265–272.

Spencer, K.A., Dee, M., Britton, P., Hiscox, J.A., 2008. Role of phosphorylation clusters in the biology of the coronavirus infectious bronchitis virus nucleocapsid protein. Virology 370, 373–381.

Tan, F., Wei, Z., Li, Y., Zhang, R., Zhuang, J., Sun, Z., Yuan, S., 2011. Identification of non-essential regions in nucleocapsid protein of porcine reproductive and respiratory syndrome virus for replication in cell culture. Virus Res. 158, 62–71.

Wang, X., Bai, J., Zhang, L., Wang, X., Li, Y., Jiang, P., 2012. Poly(A)-binding protein interacts with the nucleocapsid protein of porcine reproductive and respiratory syndrome virus and participates in viral replication. Antivirus Res. 96, 315–323.

Wootton, S.K., Rowland, R.R., Yoo, D., 2002. Phosphorylation of the porcine reproductive and respiratory syndrome virus nucleocapsid protein. J. Virol. 76, 10569–10576.

Xie, J., Christiaens, I., Yang, B., Breedam, W.V., Cui, T., Nauwynck, H.J., 2017. Molecular cloning of porcine Siglec-3, Siglec-5 and Siglec-10, and identification of Siglec-10 as an alternative receptor for porcine reproductive and respiratory syndrome virus (PRRSV). J. Gen. Virol. 98, 2030–2042.

Xie, J., Zhou, H., Cui, J., Chen, Y., Zhang, M., Deng, S., Zhou, P., Su, S., Zhang, G., 2014. Inhibition of porcine reproductive and respiratory syndrome virus by specific siRNA targeting Nsp9 gene. Infect. Genet. Evol. 28, 64–70.

Yu, J., Liu, Y., Zhang, Y., Zhu, X., Ren, S., Guo, L., Liu, X., Sun, W., Chen, Z., Cong, X., Chen, L., Shi, J., Du, Y., Li, J., Wu, J., Wang, J., 2017. The integrity of PRRSV nucleocapsid protein is necessary for up-regulation of optimal interleukin-10 through NF-kappaB and p38 MAPK pathways in porcine alveolar macrophages. Microb. Pathog 109, 319–324.

Zengel, J., Pickar, A., Xu, P., Lin, A., He, B., 2015. Roles of phosphorylation of the nucleocapsid protein of mumps virus in regulating viral RNA transcription and replication. J. Virol. 89, 7338–7347.

Zhang, M., Cao, Z., Xie, J., Zhu, W., Zhou, P., Gu, H., Sun, L., Su, S., Zhang, G., 2013. Mutagenesis analysis of porcine reproductive and respiratory syndrome virus nonstructural protein 7. Virus Genes 47, 467–477.

Zhang, Z., Yang, X., Xu, P., Wu, X., Zhou, L., Wang, H., 2017. Heat shock protein 70 in lung and kidney of specific-pathogen-free chickens is a receptor-associated protein that interacts with the binding domain of the spike protein of infectious bronchitis virus. Arch. Virol. 162, 1625–1631.